www.czasopisma.pan.pl PAN POLSKA AKADEMIA NAUK www.journals.pan.pl

A R C H I V E S O F M E T A L L U R G Y A N D M A T E R I A L S

Volume 60 2015 Issue 4

DOI: 10.1515/amm-2015-0420

M. ROZMUS-GÓRNIKOWSKA*,#, M. BLICHARSKI*

MICROSEGREGATION AND PRECIPITATES IN INCONEL 625 ARC WELD OVERLAY COATINGS ON BOILER PIPES

MIKROSEGREGACJA I WYDZIELENIA W POWŁOKACH ZE STOPU INCONEL 625 NAPAWANYCH ŁUKOWO NA RURY KOTŁOWE

The aim of this work was to investigate the microsegregation and precipitates formed due to segregation in Inconel 625 arc weld overlay coatings on boiler pipes. Examination of microsegregation and precipitates were carried out by means of a scanning electron microscope (SEM) equipped with an EDS detector as well as a transmission electron microscope (TEM) equipped with a HAADF (STEM) and an EDS detectors. The presence of precipitations in the weld overlay was also confirmed with X-ray diffraction analysis (XRD) of residue in the form of powder that remained after the electrolytic dissolution of weld overlay matrix.

The investigations showed that the interdendritic regions were considerably enriched during microsegregation with Nb, and less so with Mo. The distribution of Cr and Fe in the weld overlay is relatively uniform. The value of the partition coefficient k for Mo and Nb is lower than 1. Therefore, these elements segregate during solidification into the liquid and, once solidification is finished, the interdendritic regions are considerably enriched with these elements. The value of *k* for Cr, Ni and Fe are only slightly higher than 1. Though the Inconel 625 is a solid-solution strengthened alloy, precipitation of secondary phases occurs in weld overlays. Precipitations were identified as a Laves phase and carbonitrides (Nb, Ti)(C, N).

Keywords: microsegregation, precipitates, Inconel 625, weld overlay, SEM, TEM, STEM

Celem pracy była ocena segregacji dendrytycznej (mikrosegregacji) oraz identyfikacja wydzieleń w napoinach ze stopu Inconel 625 napawanych metodą CMT na rury kotłowe. Badania segregacji dendrytycznej oraz składu chemicznego wydzieleń w napoinach ze stopu Inconel 625 prowadzono za pomocą mikroskopu elektronowego skaningowego NanoSEM 450 firmy FEI wyposażonego w detektor EDS firmy EDAX oraz za pomocą mikroskopu elektronowego transmisyjnego (TEM, TECNAI GF20) wyposażonego w detektor HAADF do badań techniką skaningowo - transmisyjną STEM, jak również zintegrowany spektrometr promieniowania rentgenowskiego do analizy składu chemicznego firmy EDAX. Obecność wydzieleń została potwierdzona za pomocą rentgenowskiej analizy fazowej (XRD) cząstek proszku osadu uzyskanego w wyniku elektrolitycznego rozpuszczenia osnowy napoiny.

Badania wykazały, że w wyniku mikrosegregacji zachodzącej podczas krzepnięcia napoin następuje znaczne wzbogacenie obszarów międzydendrytycznych tj. obszarów między ramionami dendrytów w Nb a mniejsze w Mo. Wartość równowagowego współczynnika rozdziału *k* dla Mo i Nb jest mniejsza od 1, dlatego podczas krystalizacji pierwiastki te segregują do cieczy, a zatem, po zakończeniu krystalizacji obszary międzydendrytyczne są znacznie wzbogacone w w/w pierwiastki. Pomimo, że stop Inconel 625 jest stopem umacnianym roztworowo to w napoinach występowały wydzielenia. Na podstawie wyników analizy składu chemicznego, jak również rentgenowskiej analizy fazowej wydzielenia te zidentyfikowano jako fazę Lavesa oraz (Nb, Ti)(C, N).

1. Introduction

Resistance to corrosion is the decisive criterion for the selection of materials for construction of boiler elements for burning municipal and industrial waste due to the extremely aggressive environment of their operation. Therefore, boiler elements that operate in the most aggressive environments are usually subjected to weld overlaying with Ni alloys, in order to ensure the required operational life of boilers. The solid-solution strengthened nickel alloy Inconel 625 is widely used for welded coatings for these processes, as it is characterized by very good resistance to corrosion as well as good strength and weldability. Chromium is the element that enhances resistance to corrosion, especially in an oxidizing atmosphere. Therefore, it is the basic element of the 625 alloy. Moreover, Cr and especially Mo and Nb, provide solid-solution strengthening of the alloy [1,2].

Weld overlaying is a process of depositing a material onto a product surface by welding methods [3]. Welded coatings have a structure typical to cast metals, characterized by the fact

* AGH UNIVERSITY OF SCIENCE AND TECHNOLOGY, FACULTY OF METALS ENGINEERING AND INDUSTRIAL COMPUTER SCIENCE, AL. MICKIEWICZA 30, 30-059 KRAKOW, POLAND

Corresponding author: rozmus@agh.edu.pl

TABLE 1

Chemical composition of Inconel 625 wire, wt %

Alloy	Cr	Mo	Nb	Fe	Mn	Si	Al	C	Ni
Inconel 625	22.24	9.14	3.46	0.31	0.01	0.07	0.07	0.02	balance

that a heterogeneous solid is obtained during solidification from a homogenous liquid, as alloy components are redistributed during solidification. Redistribution of alloying elements during solidification depends on thermodynamic condition factors (the phase diagram) and solidification kinetics (diffusion, undercooling, fluid flow, etc.). Heterogeneities of the chemical composition – formed during solidification in conditions that differ from the equilibrium conditions – limited to micro-regions are referred to as microsegregation or dendritic segregation [4].

Microstructural examinations of fusion welds and Ni alloy weld overlays show that, during weld overlaying, the processes of diffusion in the weld pool as well as mixing of melted metal are sufficiently intensive for homogenisation of chemical composition of the liquid metal that corresponds to the equilibrium conditions at the solidification front. On the other hand, the diffusion in the solid phase that forms as dendrites or cells is so low – due to the *fcc* crystal structure and the high cooling rate during weld overlaying – that it becomes negligible [4]. Therefore, the formed microsegregation is satisfactorily represented by the course of solidification in the conditions, when the liquid composition is homogenous and diffusion in the solid state is negligibly small. Solidification in such conditions leads to the highest degree of microsegregation. It is also important to note that in numerous alloys, in which a eutectic transformation is not expected, the eutectic reaction in the weld overlays of these alloys was observed [2,4]. Microsegregation formed during solidification often leads to the formation of eutectics and results in a considerable widening of the alloy solidification range. Solidification of the Inconel 625 alloy starts at the temperature of about 1368 °C. The strong segregation of Nb and Mo that occurs during weld overlay solidification leads to the eutectic transformations. During the eutectic reaction, at the temperature of about 1250 °C, austenite and NbC carbides ($L_E \rightarrow \gamma$ + NbC) are formed from the liquid with eutectic composition. Similarly, at the temperature of about 1150 °C, austenite and brittle intermetallic Laves phase of the (Ni, Cr, Fe)$_2$(Nb, Mo, Ti, Si) type ($L_E \rightarrow \gamma$ + Laves phase) are formed as a result of eutectic transformation [2].

Due to the microsegregation and formation of secondary phases, corrosion resistance of a weld overlay is lower than that of a wrought material with the same but homogenous chemical composition [5,6]. Precipitation of carbides and the Laves – type phases is also disadvantageous, because ductility and fracture toughness decrease, as the amount of these phases increases. Moreover, susceptibility to solidification and liquation cracking increases [7,8].

The aim of this work was to investigate the microsegregation and precipitates formed due to segregation in Inconel 625 arc weld overlay coatings on boiler pipes.

2. Material and experimental procedure

The research was focused on Inconel 625 weld overlays on 16Mo3 steel boiler pipes. Weld overlays were produced by circumferential weld overlaying by the Cold Metal Transfer (CMT) method [9,10,22]. The solid-solution strengthened Inconel 625 alloy in the form of 1 mm in diameter wire was used in weld overlaying. The chemical composition of Inconel 625 used for weld overlaying and the 16Mo3 steel substrate is shown in Tables 1 and 2 respectively.

TABLE 2

Chemical composition of 16Mo3 steel, wt %

Steel	C	Si	Mn	Cr	Mo	Ni	Fe
16Mo3	0.16	0.34	0.65	0.30	0.30	0.30	balance

The microstructure and microsegregation (dendritic segregation) of weld overlays were examined on cross-sections parallel to the pipe axis and perpendicular to the pipe surface. The metallographic samples of weld overlays, were polished with diamond abrasive pastes and then subjected to electrolytic etching with a 10 % solution of CrO_3 in H_2O at room temperature, at a voltage of 1.8 V for 15 s. Examinations were performed with the FEI NanoSEM 450 electron scanning microscope, equipped with an EDAX EDS detector. To reveal and assess microsegregation, point to point analysis of the chemical composition was performed. The analysis comprised 100 measurements along a straight line perpendicular to the direction of cellular dendritic growth and ran across several dendrites. The line along which measurements were carried out was 16.5 µm long, while successive measurements were spaced every 0.17 µm. The results acquired were used to construct diagrams showing the distribution of the selected elements - i.e. Mo, Nb, Cr, Ni and Fe (wt %) – as a function of measuring distance. Moreover, Mo, Nb, Cr and Ni distribution maps were prepared for selected areas that covered several dendrites and interdendritic regions.

The value of the partition coefficient k for Mo, Nb, Cr, Fe and Ni was determined by dividing the calculated average content of a given element in dendrite cores (C_s) by its average content in the measurement area (C_o) ($k = C_s/C_o$). The average content of a given element in dendrite cores was calculated on the basis of individual measurements of composition in the dendrite cores. The average content of a given element in the measurement area was evaluated on the basis of the chemical composition analysis performed for the weld overlay area covering all the measurements in dendrite cores.

Examinations of weld overlay microstructure and microsegregation of chemical composition were also carried out by means of a transmission electron microscope (TEM, TECNAI GF20) equipped with a HAADF detector for scanning

transmission electron microscopy (STEM) examinations and with an integrated X-ray spectrometer (manufactured by EDAX) for analysing chemical composition. Thin foils for TEM examinations were prepared by FIB (Focus Ion Beam). The foils were excised from a pipe cross-section parallel to the pipe axis and perpendicular to the pipe surface. Chemical composition analyses were performed along straight lines perpendicular to the direction of cellular dendritic growth, in order to assess microsegregation. The analysis covered two interdendritic regions. Mo, Nb, Cr, and Ni distribution maps were collected for selected areas containing precipitations.

In order to determine the chemical composition of the precipitates appearing in the interdendritic regions, qualitative and quantitative point analyses were performed by means of X-ray spectroscopy with energy dispersion (SEM/TEM/EDS).

Additionally, the weld overlay matrix was dissolved by the electrolytic method and the resultant residue in the form of powder was subjected to quantitative analysis of chemical composition (SEM/EDS). Moreover, both the residue powder and the weld overlay were subjected to X-ray diffraction analysis (XRD). XRD examinations were performed by means of an Empyrean DY 1061 PANalytical X-ray diffractometer using Cu radiation. The analysis was carried out in the Bragg-Brentano geometry. The sample subjected to XRD analysis was excised parallel to the pipe axis and perpendicular to the pipe diameter.

3. Results and discussion

A detailed discussion of microstructural zones appearing in weld overlays (the fusion zone, the partially mixed zone, the heat affected zone and the base material) and results of the analysis of chemical composition of particular weld overlay regions are presented in Ref. [9, 10].

Fig. 1 shows an example of weld overlay microstructure with a marked line, perpendicular to the cellular dendritic growth direction. A local analysis of chemical composition was carried out along this line, in order to assess the microsegregation of elements during solidification process. The figure also shows diagrams of variations in the concentration (content) of the analysed elements – Mo, Nb, Cr, Ni and Fe (% by weight) – along the above-mentioned line. Fig. 2 and Fig. 3 show maps obtained by SEM/EDS and TEM/EDS, respectively – of Mo, Nb, Cr and Ni distributions in the selected weld overlay region. An analysis of the chemical composition showed that during solidification the interdendritic regions - i.e. the regions between dendrite arms – were considerably enriched with Nb and less with Mo. The distribution of Cr and Fe in the weld overlay was relatively uniform. Similar distribution of elements in an Inconel 625 weld overlay were obtained by Cieslak [11-13], DuPont [14-16] and Silva [17]. The lighter regions on the Nb and Mo distribution maps (SEM/EDS) correspond to interdendritic regions enriched with Mo and Nb (Fig. 1). On the other hand, the very small, bright regions that are visible in the interdendritic regions on the Nb and Mo distribution maps (TEM/EDS) are considerably enriched with Mo and Nb, while they are also considerably depleted of Cr and Ni. These regions were identified as precipitates.

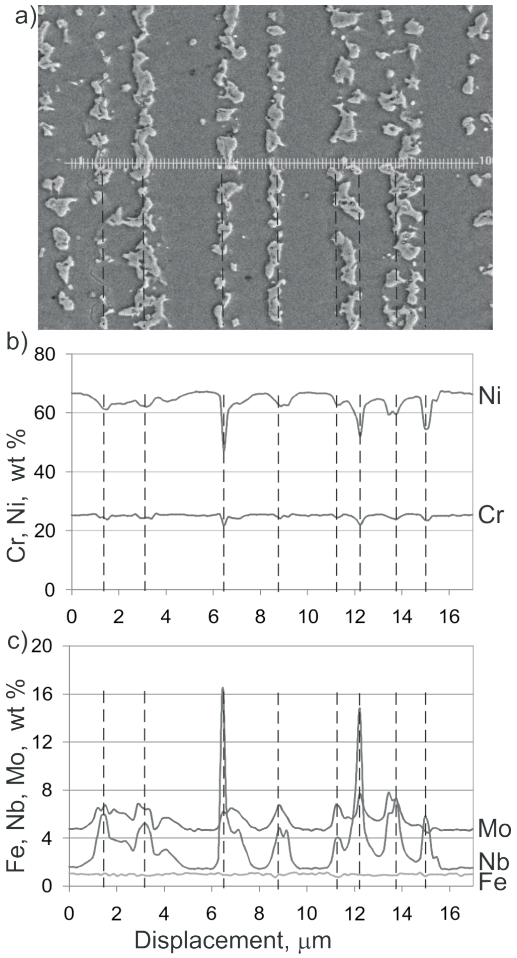

Fig. 1. Microstructure of the weld overlay (a) and the line profile of the Ni, Cr (b) and Mo, Nb, Fe (c) along the dashed line on microstructure

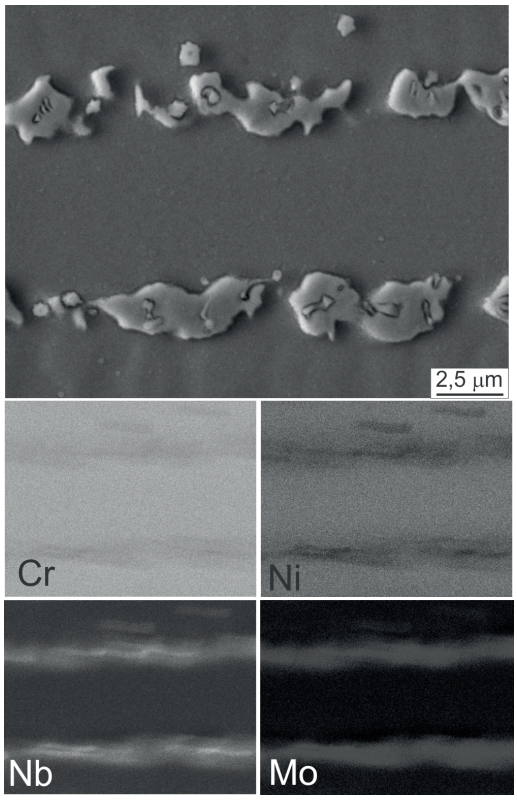

Fig. 2. The maps of particular elements distribution obtained by SEM/EDS

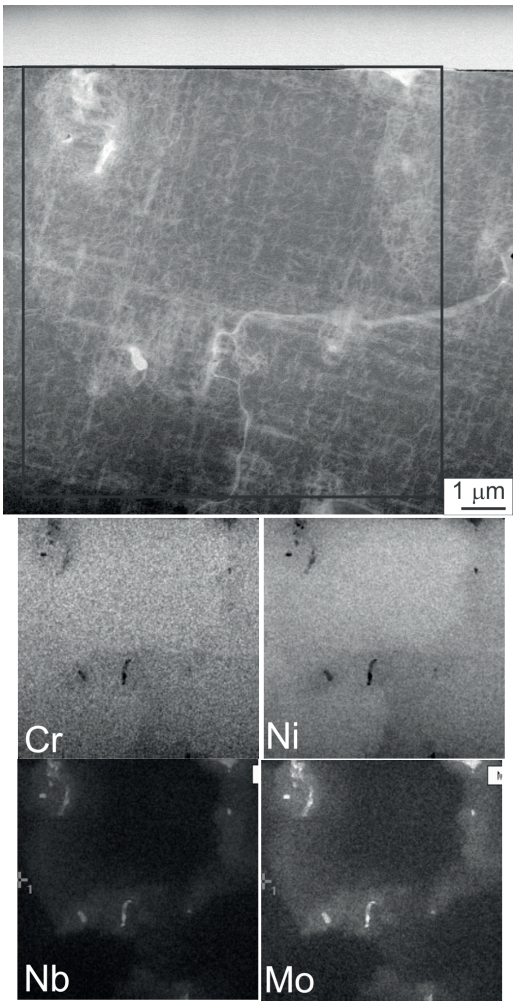

Fig. 3. The maps of particular elements distribution obtained by TEM/EDS

Table 3 shows the average content of particular elements in dendrite cores (C_s) and their average content in the analyzed area (C_o) as well as the values of the partition coefficient k for particular elements. The values of the partition coefficient calculated for Nb and Mo are 0.55 and 0.88 respectively. The values calculated for Cr, Ni and Fe, are greater than 1 and are equal to 1.01, 1.03 and 1.25 respectively. Since values of k for Mo and Nb are lower than 1, these elements segregate during solidification into the liquid and, once solidification is finished, the interdendritic regions are considerably enriched with these elements. It is worth noting that the obtained results are close to the data found in the relevant literature k_{Nb}=0.49; k_{Mo}= 0.89; k_{Ni}=1.04; k_{Fe}=1.14; k_{Cr}=1.05) [17].

TABLE. 3

The average content of particular elements in dendrite cores (C_s), and their average content in the analyzed area (C_o), as well as the partition coefficient k for Mo, Nb, Cr, Ni and Fe

Element	C_s	C_o	k
Mo	7.89	8.95	0.88
Nb	1.99	3.60	0.55
Cr	23.60	23.33	1.01
Ni	64.76	62.47	1.03
Fe	1.90	1.52	1.25

Banovic [7] and DuPont [2] showed that, in the case of Ni-based weld overlays, the content of Fe in a particular alloy has a high impact on the value of the partition coefficient k for Nb and Mo. The higher the content of Fe in a weld overlay, the lower the value of the partition coefficient k for Nb and Mo. It means that the segregation of these elements is stronger. The increasing value of the partition coefficient k for Nb and Mo, coupled with an increase of the Fe content in the alloy, likely results from a substantial difference in solubility of Nb and Mo in Ni and Fe-γ [2, 7]. The highest solubility of Nb in Ni reaches the value of about 18 wt % (at 1286 °C), while the maximum solubility of Nb in Fe-γ is only 1.5 wt % (at 1210 °C). Also, the solubility of Mo in Ni approaches the value of about 35 wt % (at 1200 °C), while the maximum solubility of Mo in Fe-γ does not exceed the value of 2 wt % (at 1150 °C). By reducing the solubility of Nb and Mo in Ni, Fe simultaneously decreases the value of the partition coefficient k for these elements. The increased content of Fe in the weld overlay is primarily due to melting and dissolution of the base material. Therefore, in order to reduce Nb and Mo segregation in Ni-based weld overlays, i.e. to increase the value of the partition coefficient k for these elements, the melted portion of the substrate material should be as small as possible. This can be achieved by selecting an appropriate weld overlaying method and process parameters.

Microstructural examinations performed by means of a scanning electron microscope showed that, in spite of the fact that the Inconel 625 alloy belongs to solid-solution strengthened alloys, numerous precipitates were found in weld overlays. Precipitation occurred only in the spaces between dendrites and cells, i.e. in the regions enriched with Nb and Mo. Two types of precipitates were distinguished according to their shape: elongated, oval precipitates and tiny, angular and sharp-edged ones resembling parallelograms (Fig. 4). Shapes of the precipitates revealed in TEM are shown in Fig. 5. Figure 6 shows the results of the linear chemical analysis (TEM/EDS) carried out along the direction perpendicular to the dendrite

TABLE 4

Phase compositions (wt %) – precipitates (SEM/EDS), (Nr 1, 2, 6 and from analyses, nr 3, 4 and 5 from literature)

Nr	Phase	Compositions, wt %					
		Nb	Mo	Ti	Cr	Fe	Ni
1	Laves	15.56	13.39	0.30	15.76	10.75	43.52
2	Laves	14.52	9.29	0.71	17.59	12.29	45.25
3	Cieslak (Laves)	16.8-19.2	17.6-19.8	not analyzed	13.6-15.6	0.9-1.4	45.6-48.2
4	Floren (Laves)	11	12	not analyzed	22	3	48
5	DuPont (Laves)	22.1	16.7	not analyzed	11.6	18	30.2
6	(Nb, Ti)(C, N)	27.47	8.16	5.92	14.93	10.18	32.78
7	(Nb, Ti)(C, N)	31.69	8.91	5.42	13.86	9.39	30.18

growth and crossing two interdendritic regions. The line along which the analysis of chemical composition was performed (marked with a "1" in Fig. 6) was obtained in the region where precipitates were visible. On the other hand the line marked with a "2" crossed the zone where precipitates were not observed. The analysis showed that the content of Nb and Mo in precipitates is higher than in the interdendritic regions. During weld overlay solidification, the austenite dendrite cores that form at the very beginning of the solidification process are depleted of Mo and Nb. The precipitates form in the interdendritic regions as a result of the eutectic reaction, only after the liquid becomes enriched with Mo and Nb. According to Ref. [2, 8] the solidification process of the Inconel 625 proceeds as follows: L → L + γ → L + γ + NbC → L + γ + NbC + Laves phase → γ + NbC + Laves phase.

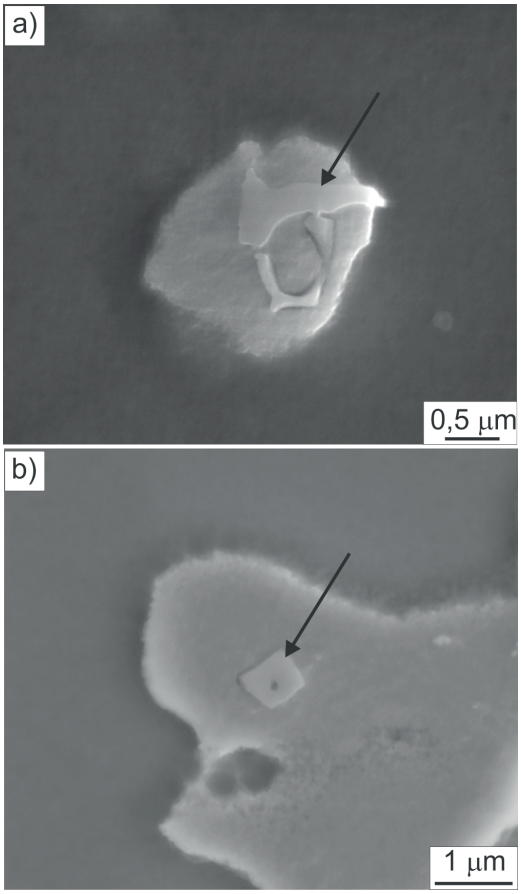

Fig. 4. SEM micrographs showing the main morphologies of secondary phases: elongated one (a) and parallelogram shaped (b); precipitates are indicated by arrows

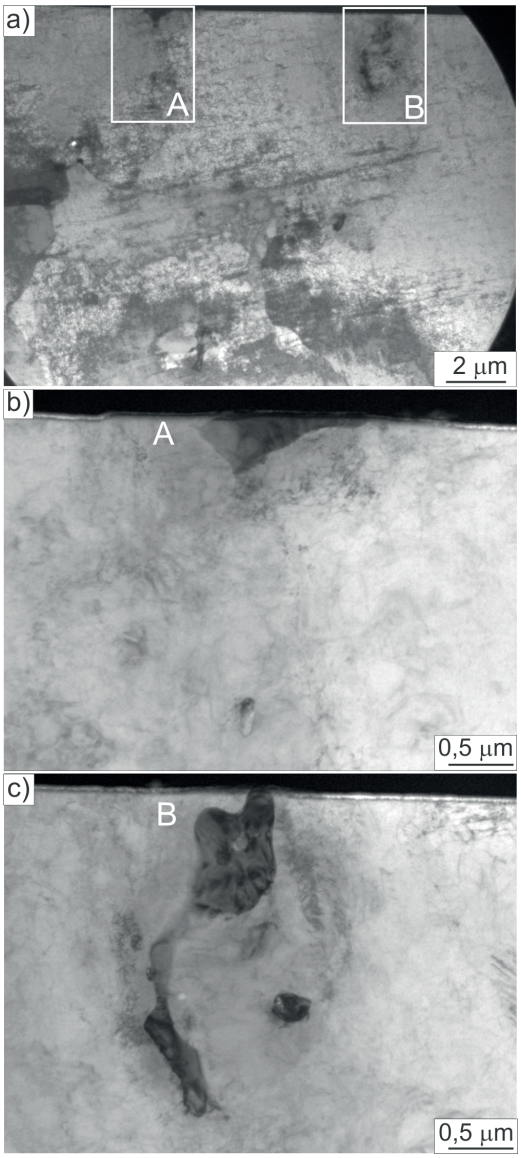

Fig. 5. TEM images showing precipitates in the interdendritic regions

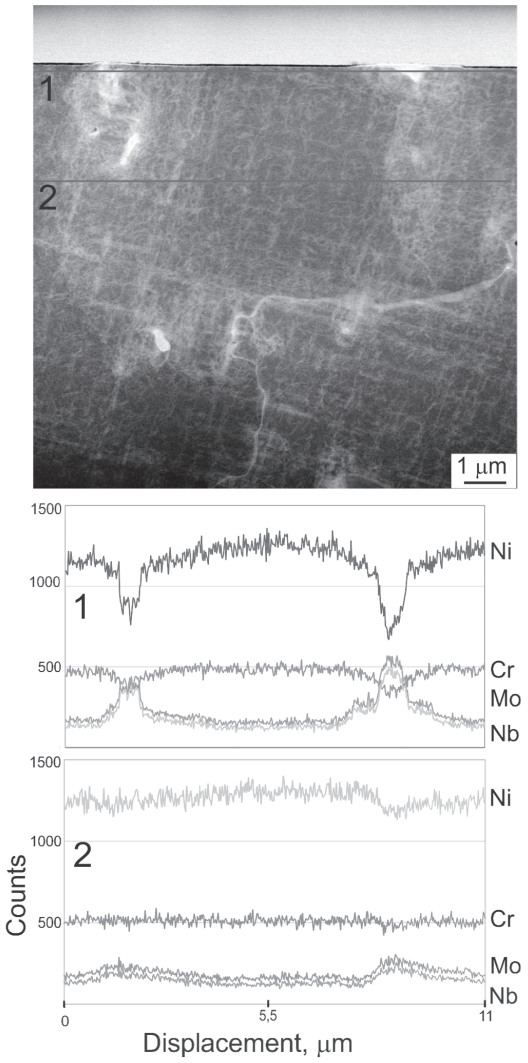

Fig. 6. Microstructure of the weld overlay and the results of the linear analysis of chemical composition (TEM/EDS) carried out along lines 1 and 2

The results of the quantitative analysis of the chemical composition (SEM/EDS) of precipitates are presented in Table 4. For comparison, this table also includes the chemical composition of the Laves phase in weld overlays examined by Cieslak [8], Floren [18] and DuPont [19]. This analysis showed that the elongated phase was enriched in Mo and Nb, and simultaneously it contained low amounts of such elements as Ni, Cr and Fe that do not segregate to interdendritic areas. These experimental results together with the data presented in References [8,18] allow for the identification of these precipitates as an intermetallic Laves phase. The Laves phase exhibits a hexagonal crystal structure and is characterized by A_2B stoichiometric composition, where A stands for Ni, Fe and Cr, while B stands for Nb, Mo, Ti and Si. It is worth noting that the results acquired in the present study are consistent with the results presented by DuPont [2, 14-16], Silva [17] and Maguire [21]. It was also found that precipitates in the shape of a parallelogram contain much more Ti than the formerly discussed elongated precipitations. Considering both the chemical composition and particle shape, as well as data presented by Maguire [21] and Silva [17] precipitates in the shape of a parallelogram were identified as carbonitrides (Nb, Ti)(C, N) (Table 4).

TABLE 5

Phase compositions (wt %) - powders after matrix electrolytic dissolution (SEM/EDS)

Nr	Phase compositions (wt %)					
	Nb	Mo	Ti	Cr	Fe	Ni
1	49.07	37.27	1.55	9.58	0,49	2,04
2	42.37	39.61	1.80	9.16	0,91	6,15
3	21.49	19.93	0.78	15.73	2,57	3,11
4	20.20	19.17	0.65	16.28	2,65	41,04

The presence of two types of precipitates was also confirmed by quantitative analysis of chemical composition (SEM/EDS) of the powder residue that remained after the electrolytic dissolution of the weld overlay matrix (Table 5). The analysis identified the presence of Mo and Nb-rich particles, that contained less than 1% of Ti (Laves phase) and of particles with clearly increased Nb content (even 49 %), that were simultaneously characterized by Ti content above 1% (Nb, Ti)(C, N).

As the volume fraction of precipitates was small, X-ray diffraction analysis (XRD) of the coating reveals only the presence of Ni-base solid solution in the weld overlay. However, all peaks were shifted from their theoretical positions (for pure Ni) in the direction of higher values of the angle θ. This is due to the presence of alloy elements that alter the parameter of the solid solution crystal structure (Fig. 7). The X-ray diffractogram taken from the weld overlay also showed that the coating was highly textured. It was demonstrated by apparent higher intensity of {200} reflection in the overlay than in the theoretical, un-textured diffractogram. The reason for this texturing is the directional solidification that occurs as a result of directional heat removal during weld overlaying. It is well established that in materials with the fcc (*cF*4) crystal structure, grains with the <100> direction parallel to the heat removal direction grow at the fastest rate.

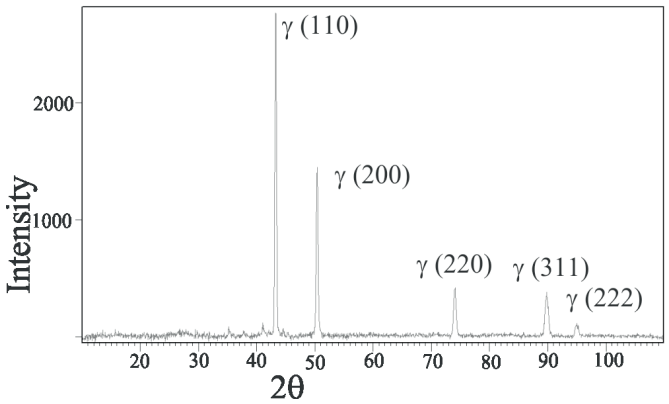

Fig.7. X-ray diffractogram of the Inconel 625 weld overlay

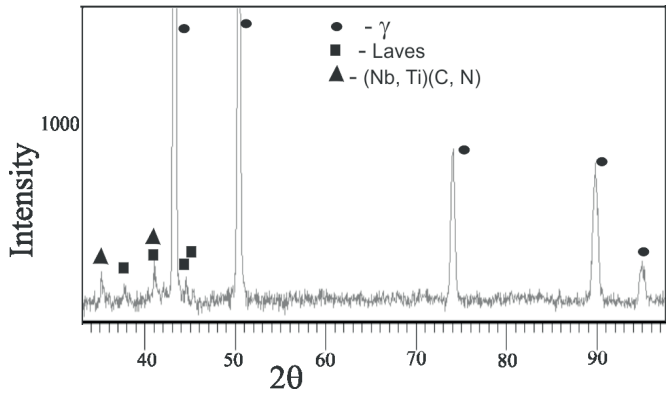

Fig.8. X-ray diffractogram of the powders after electrolityc dissolution

The X-ray diffraction analysis of particles of the power residue that remained after the electrolytic dissolution of the weld overlay matrix, revealed the peaks coming from the Laves phase as well as carbonitride in addition to Ni solid solution peaks (Fig. 8). In the diffractogram of the sediment powder, one can not only observe clear peaks generated by the base (Ni-base solid solution), but also weaker peaks originating from the Laves phase and carbonitrides of the (Nb, Ti)(C, N) type.

4. Conclusions:

- Solidification of weld overlays brings about substantial microsegregation of Nb and Mo. The interdendritic regions, i.e. the regions between dendrite arms, are considerably enriched with Nb, and less so with Mo. The distribution of Cr in the weld overlay is relatively uniform.
- The value of the partition coefficient *k* for Mo and Nb is lower than 1. Therefore, these elements segregate during solidification into the liquid and, once solidification is completed, the interdendritic regions are considerably enriched with these elements.
- Though the Inconel 625 is a solid-solution strengthened alloy, the precipitates of secondary phases occurs in weld overlays. Precipitates developed only in spaces between dendrites and cells, i.e. in the regions enriched with Nb and Mo.
- Considering the chemical composition, shape and XRD analysis of the residue in the form of powder that remained after the electrolytic dissolution, precipitates were identified as Laves phase and carbonitrides (Nb, Ti)(C, N).

Acknowledgements

The project was financed by National Science Center; grant number DEC-2011/01/D/ST8/04948.

Highlights

- the microsegregation and precipitates in Inconel 625 arc weld overlay were investigated
- during microsegregation the interdendritic regions were enriched with Nb and Mo
- precipitations were identified as a Laves phase and carbonitrides (Nb, Ti)(C, N)

REFERENCES

[1] M. Montgomery, A.N. Hansson, S.A. Jensen, T. Vilhelmsen, N.H. Nielsen, Materials and Corrosion **62**, 1-12 (2011).
[2] J.N. DuPont, J.C. Lippold, S.D Liser, Welding metallurgy and weldability nickel base alloys, A John Wiley & Sons, INC., Publication, 2009.
[3] J.F. Lancaster, Metallurgy of welding, Abington Publishing, Cambridge 1999.
[4] S. Kou, Welding Metallurgy, A John Wiley & Sons, INC., Publication, New Jersey 2003.
[5] H.R. Zareie Rajani, S.A.A. Akbari Mousavi, F. Madani Sani, Materials and Design **43**, 467-474 (2013).
[6] J.N. DuPont, A. W. Stockdale, A. Caizza, A. Esposito, Welding Journal **92**, 218-225 (2013).
[7] S.W. Banovic, J.N. DuPont, A.R. Marder, Science and Technology of welding and Joining **7**, 374-383 (2002).
[8] M.J. Cieslak. T.J. Headley, T Kollie, A.D. Romig, Metallurgical Transactions A **19A**, 1988-2319 (1987).
[9] M. Rozmus-Górnikowska, M. Blicharski, J. Kusiński, L. Kusiński, M. Marszycki, Archives of Metallurgy 58, 1093-1096 (2013).
[10] M. Rozmus-Górnikowska, M. Blicharski, J. Kusiński, Metallic Materials 52, 141-147 (2014).
[11] M.J. Cieslak, T.J. Headley, R.B. Frank, Welding Research Supplement, 473-482 (1989).
[12] M.J. Cieslak, The metallurgy of alloy 625. Superalloys 718, 625 and Various Derivatives, The Minerals, Metals and Materials Society, Pennsylvania 1991.
[13] M.J. Cieslak, Welding Research Supplement, 49-56 (1987).
[14] J.N. DuPont, Metallurgical and Materials Transactions A. **27A**, 3612-3620 (1996).
[15] J.N. DuPont, S.W. Banovic, A.R. Marder, Supplement to the Welding Journal, 125-135 (2003).
[16] J.N. DuPont, C.V Robino, A.R. Marder, M.R. Notis, Metallurgical and Materials Transactions A. **29A,** 2797-2805 (1998).
[17] C.C Silva, H.C. de Miranda, M.F. Motta, J.P Farias, C.R.M. Afonso, A.J. Ramires, Journal of Materials Research and Technology 2, 228-237 (2013).
[18] S. Floreen, G.E. Fuschs, W.J. Yang, The metallurgy of alloy 625. Superalloys 718, 625 and Various Derivatives, The Minerals, Metals and Materials Society, Pennsylvania 1991.
[19] J.N. DuPont, C.V Robino, J.R. Michael, M.R. Notis, A.R. Marder, Metallurgical and Materials Transactions A. 29A, 2785-2796 (1998).
[20] F. Cortial, J. M. Corrieu, Ch. Vernot-Loier, Heat treatments of weld alloy 625: influence on the microstructure, mechanical properties and corrosion resistance, Superalloys 718, 625 and Various Derivatives. The Minerals, Metals and Materials Society, Pennsylvania (1994).
[21] M.C. Maguire, J.R. Michael, Weldability of alloy 718, 625 and variants. Superalloys 718, 625 and Various Derivatives, The Minerals, Metals and Materials Society, Pennsylvania (1994).
[22] M. Rozmus-Górnikowska, Ł. Cieniek, M. Blicharski, J. Kusiński, Archives of Metallurgy 59, 1081-1084 (2014).

Received: 10 February 2015.